

Properties of Coupled Single-Electron Lines

1st Krzysztof Pomorski

University College Dublin

School of Electrical and Electronic Engineering

Dublin, Ireland

email: kdpomorski@gmail.com

2nd Panagiotis Giounanlis

University College Dublin

School of Electrical and Electronic Engineering

Dublin, Ireland

email: panagiotis.giounanlis@ucd.ie

3rd Elena Blokhina

University College Dublin

School of Electrical and Electronic Engineering

Dublin, Ireland

email: elena.blokhina@ucd.ie

4th Andrew Mitchell

University College Dublin

School of Physics

Dublin, Ireland

email: andrew.mitchell@ucd.ie

5th Imran Bashir

Equal 1

Dublin, Ireland

email: imran.bashir@equal1.com

6th Dirk Leipold

Equal 1

California, USA

email: dirk.leipold@equal1.com

7th Robert Staszewski

University College Dublin, School of Electrical and Electronic Engineering

Dublin, Ireland

email: robert.staszewski@ucd.ie

Abstract—Fundamental properties of two electrostatically interacting single-electron lines (SEL) are determined from a minimalistic tight-binding model. The lines are represented by a chain of coupled quantum wells that could be implemented in a mainstream nanoscale CMOS process technology and tuned electrostatically by DC or AC voltage biases. The obtained results show an essential qualitative difference with two capacitively coupled classical electrical lines. The derived equations and their solutions prove that the two coupled SET lines can create an entanglement between electrons. The results indicate a possibility of constructing electrostatic (non-spin) coupled qubits that could be used as building blocks in a CMOS quantum computer.

Index Terms—tight-binding model, Single Electron Lines (SEL), quantum phase transition, entanglement, insulator-metallic transition, electrostatic interaction, two-body problem, programmable quantum matter, quantum transport, single electron transistor

I. TECHNOLOGICAL MOTIVATION

The CMOS electronic devices continue to scale down with Moore's law and now are starting to reach the fundamental limitation dictated by the fact that the electron charge is quantized [2], [6]. Moreover, it is commonly accepted by the technologists that the use of fractional electron charge has no practical meaning. On the other hand, the use of different representation of information as by fluxons (quantized flux of magnetic field) in Rapid Single Quantum Flux electronics turns out to have its limitations from the point of view of its size, as implementation in very large scale integration circuits [1]. In this work, we limit ourselves to the electrostatic description of an electron-electron interaction. Current cryogenic CMOS technology development opens perspectives in implementation of CMOS quantum computer [6] or use of cryogenic CMOS as interface to superconducting quantum circuits [2].

Fundamentally, the electron quantum properties are captured by the Schrödinger equation that can be obtained in the case of a single electron in effective potential or in the case of many-

electron system confined by some local potential. However, the Schrödinger equation in a continuous position space is not the most straightforward approach to capture all electron transport properties on discrete lattices present in various types of metamaterials that can be manufactured on large scale. In this work, we use a tight-binding approximation that can be derived from the Schrödinger equation [10].

II. MATHEMATICAL STATEMENT OF THE PROBLEM

At first, we consider a physical system of an electron confined in a potential with two minima, as depicted in Fig. 2(A), which was also considered by Fujisawa [4] and Petta [8]. We can write the Hamiltonian in the second quantization as

$$\hat{H} = \sum_{i,j} t_{i \rightarrow j} \hat{a}_i^\dagger \hat{a}_j + \sum_i E_{pi} \hat{a}_i^\dagger \hat{a}_i + \sum_{i,j,k,l} \hat{a}_i^\dagger \hat{a}_j^\dagger \hat{a}_i \hat{a}_j V_{i,j}, \quad (1)$$

where \hat{a}_i^\dagger is a fermionic creator operator at i -th point in the space lattice and \hat{a}_j is fermionic annihilator operator at j -th point of the lattice. The hopping term $t_{i \rightarrow j}$ describes hopping from i -th to j -th lattice point and is a measure of kinetic energy. The potential $V_{i,j}$ represents particle-particle interaction and term E_{pi} incorporates potential energy. In this approach we neglect the presence of a spin. It is convenient to write a system Hamiltonian in spectral form as

$$\begin{aligned} \hat{H}(t) = & E_{p1}(t) |1, 0\rangle \langle 1, 0| + E_{p2}(t) |0, 1\rangle \langle 0, 1| + \\ & t_{1 \rightarrow 2}(t) |0, 1\rangle \langle 1, 0| + t_{2 \rightarrow 1}(t) |1, 0\rangle \langle 0, 1| = \\ & = \frac{1}{2}(\hat{\sigma}_0 + \hat{\sigma}_3)E_{p1}(t) + \frac{1}{2}(\hat{\sigma}_0 - \hat{\sigma}_3)E_{p2}(t) + \\ & \frac{1}{2}(\hat{\sigma}_1 - i\hat{\sigma}_2)t_{2 \rightarrow 1}(t) + \frac{1}{2}(i\hat{\sigma}_2 - \hat{\sigma}_1)t_{1 \rightarrow 2}(t) \end{aligned} \quad (2)$$

where Pauli matrices are $\hat{\sigma}_0, \dots, \hat{\sigma}_3$ while system quantum state is given as $|\psi(t)\rangle = \alpha(t) |1, 0\rangle + \beta(t) |0, 1\rangle$ with $|\alpha|^2 + |\beta|^2 = 1$ and is expressed in Wannier function eigenbases $|1, 0\rangle =$

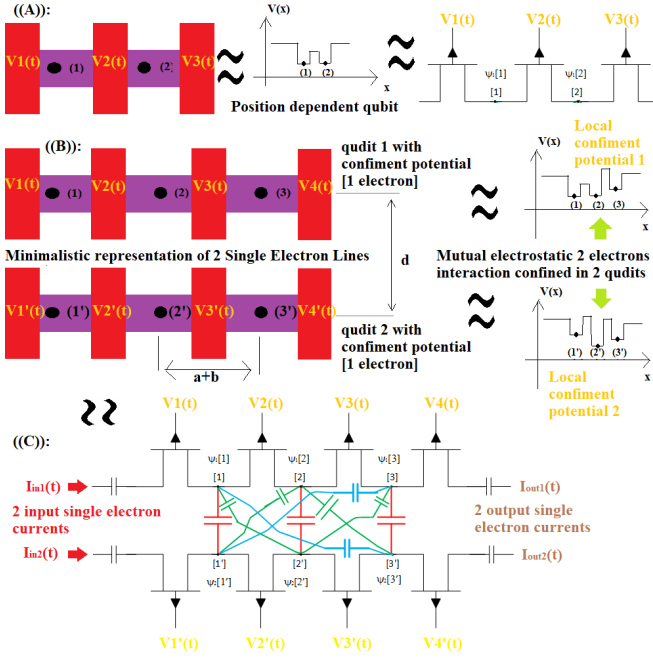


Fig. 1. Nanometer CMOS structure, effective potential and circuit representation of: (A) electrostatic position-dependent qubit [5]; (B)–(C) two electrostatic position-dependent qudits representing two inductively interacting lines (upper ‘u’ and lower ‘l’ quantum systems) in minimalistic way (more rigorously they shall be named as MOS transistor single-electron lines). Presented systems are subjected to the external voltage biasing that controls the local potential landscape in which electrons are confined.

$w_L(x)$ and $|0, 1\rangle = w_R(x)$ which underlines the presence of electron on the left/right side as equivalent to picture from Schrödinger equation [5]). We obtain two energy eigenstates

$$|E_{1(2)}\rangle = \left(\frac{(E_{p2} - E_{p1}) \pm \sqrt{4t_{1 \rightarrow 2} t_{2 \rightarrow 1} + |E_{p1} - E_{p2}|^2}}{2t_{1 \rightarrow 2}} \right) = \frac{(E_{p2} - E_{p1}) \pm \sqrt{4t_{1 \rightarrow 2} t_{2 \rightarrow 1} + |E_{p1} - E_{p2}|^2}}{2t_{1 \rightarrow 2}} |1, 0\rangle + |0, 1\rangle.$$

and energy eigenvalues

$$E_{1(2)} = \frac{1}{2}(E_{p1} + E_{p2} \pm \sqrt{4t_{1 \rightarrow 2} t_{2 \rightarrow 1} + |E_{p1} - E_{p2}|^2}). \quad (3)$$

The eigenstate depends on an external vector potential source acting on the qubit by means of $t_{1 \rightarrow 2} = |t_{1 \rightarrow 2}|e^{i\alpha}$. Since every energy eigenstate is spanned by $|0, 1\rangle$ and $|1, 0\rangle$, we will obtain oscillations of occupancy between two wells [5], [6]. It is worth-mentioning that the act of measurement will affect the qubit quantum state. Since we are dealing with a position-based qubit, we can make measurement of the electron position with the use an external single-electron device (SED) in close proximity to the qubit. This will require the use of projection operators that represent eigenenergy measurement as $|E_{0(1)}\rangle \langle E_{0(1)}|$ or, for example, measurement of the electron position at left side so we use the projector $|1, 0\rangle \langle 0, 1|$. We can extend the model for the case of three

(and more) coupled wells. In such a case, we obtain the system Hamiltonian for a position based qudit:

$$\hat{H} = \sum_s E_{ps} |s\rangle \langle s| + \sum_{l, s, s' \neq l} t_{s \rightarrow l} |l\rangle \langle s|, \quad (4)$$

where $|1\rangle = |1, 0, 0\rangle$, $|2\rangle = |0, 1, 0\rangle$, $|3\rangle = |0, 0, 1\rangle$ and its Hamiltonian matrix and quantum state $|\psi\rangle$ (with a normalization condition $|\alpha|^2 + |\beta|^2 + |\gamma|^2 = 1$) is given as

$$H(t) = \begin{pmatrix} E_{p1}(t) & t_{2 \rightarrow 1}(t) & t_{3 \rightarrow 1}(t) \\ t_{1 \rightarrow 2}(t) & E_{p2}(t) & t_{3 \rightarrow 2}(t) \\ t_{1 \rightarrow 3}(t) & t_{2 \rightarrow 3}(t) & E_{p3}(t) \end{pmatrix},$$

$$|\psi\rangle = \begin{pmatrix} \alpha(t) \\ \beta(t) \\ \gamma(t) \end{pmatrix} = \alpha(t) |1, 0, 0\rangle + \beta(t) |0, 1, 0\rangle + \gamma(t) |0, 0, 1\rangle.$$

Coefficients $\alpha(t)$, $\beta(t)$ and $\gamma(t)$ describe oscillations of occupancy of one electron at wells 1, 2 and 3. The problem of qudit equations of motion can be formulated by having $|\psi\rangle = c_1(0)e^{-\frac{i}{\hbar}tE_1}|E_1\rangle + c_2(0)e^{-\frac{i}{\hbar}tE_2}|E_2\rangle + c_3(0)e^{-\frac{i}{\hbar}tE_3}|E_3\rangle$, where $|c_1(0)|^2$, $|c_2(0)|^2$ and $|c_3(0)|^2$ are probabilities of occupancy of E_1 , E_2 and E_3 energetic levels. Energy levels are roots of 3rd order polynomial

$$(-E_{p1}E_{p2}E_{p3} + E_{p3}t_{12}^2 + E_{p1}t_{23}^2 + (E_{p1}E_{p2} + E_{p1}E_{p3} + E_{p2}E_{p3} - t_{12}^2 - t_{23}^2)E - (E_{p1} + E_{p2} + E_{p3})E^2 + E^3 = 0, \quad (5)$$

where $|E_1\rangle$, $|E_2\rangle$, $|E_3\rangle$ are 3-dimensional Hamiltonian eigenvectors.

By introducing two electrostatically interacting qudits, we are dealing with the Hamiltonian of the upper and lower lines as well as with their Coulomb electrostatic interactions. We are obtaining the Hamiltonian in spectral representation acting on the product of Hilbert spaces in the form of

$$\hat{H} = \hat{H}_u \times I_l + I_u \times \hat{H}_l + \hat{H}_{u-l} \quad (6)$$

where H_u and H_l are Hamiltonians of separated upper and lower qudits, H_{l-u} is a two-line Coulomb interaction and $I_{u(l)} = |1, 0, 0\rangle_{u(l)} \langle 1, 0, 0|_{u(l)} + |0, 1, 0\rangle_{u(l)} \langle 0, 1, 0|_{u(l)} + |0, 0, 1\rangle_{u(l)} \langle 0, 0, 1|_{u(l)}$. The electrostatic interaction is encoded in $E_c(1, 1') = E_c(2, 2') = E_c(3, 3') = \frac{e^2}{4\pi\epsilon_0\epsilon_d} = q_1$ (red capacitors of Fig.1) and $q_2 = \frac{e^2}{4\pi\epsilon_0\epsilon_d} = E_c(2, 1') = E_c(2, 3') = E_c(1, 2') = E_c(3, 2') = \frac{e^2}{4\pi\epsilon_0\epsilon_d\sqrt{d^2 + (a+b)^2}}$ and electrostatic energy of green capacitors of Fig.1. is

$$E_c(1, 3') = E_c(3, 1') = q_2 = \frac{e^2}{4\pi\epsilon_0\epsilon_d\sqrt{d^2 + 4(a+b)^2}}, \quad (7)$$

where a , b and d are geometric parameters of the system, e is electron charge and ϵ is a relative dielectric constant of the material; ϵ_0 corresponds to the dielectric constant of vacuum. The very last Hamiltonian corresponds to the following quantum state $|\psi(t)\rangle$ ($|\gamma_1(t)|^2 + \dots + |\gamma_9(t)|^2 = 1$) given as

$$|\psi(t)\rangle = \gamma_1(t) |1, 0, 0\rangle_u |1, 0, 0\rangle_l + \gamma_2(t) |1, 0, 0\rangle_u |0, 1, 0\rangle_l + \gamma_3(t) |1, 0, 0\rangle_u |0, 0, 1\rangle_l + \gamma_4(t) |0, 1, 0\rangle_u |1, 0, 0\rangle_l + \gamma_5(t) |0, 1, 0\rangle_u |0, 1, 0\rangle_l + \gamma_6(t) |0, 1, 0\rangle_u |0, 0, 1\rangle_l + \gamma_7(t) |0, 0, 1\rangle_u |0, 0, 1\rangle_l + \gamma_8(t) |0, 0, 1\rangle_u |0, 1, 0\rangle_l + \gamma_9(t) |0, 0, 1\rangle_u |0, 0, 1\rangle_l, \quad (8)$$

where $|\gamma_1(t)|^2$ is the probability of finding two electrons at nodes 1 and 1' at time t (since γ_1 spans $|1, 0, 0\rangle_u |1, 0, 0\rangle_l$), etc. The Hamiltonian has nine eigenenergy solutions that are parametrized by geometric factors and hopping constants $t_{k,m}$

as well as energies $E_p(k)$ for the case of 'u' or 'l' system. Formally, we can treat $E_{pk} = t_{k \rightarrow k} \equiv t_{k,k} \equiv t_k \in \mathbf{R}$ as a hopping from k -th lattice point to the same lattice point k . We obtain the following Hamiltonian

$$\hat{H} = \begin{pmatrix} \xi_{1,1'} & t_{1' \rightarrow 2'} & t_{1' \rightarrow 3'} & t_{1 \rightarrow 2} & 0 & 0 & t_{1 \rightarrow 3} & 0 & 0 \\ t_{2' \rightarrow 1'} & \xi_{1,2'} & t_{2' \rightarrow 3'} & 0 & t_{1 \rightarrow 2} & 0 & 0 & t_{1 \rightarrow 3} & 0 \\ t_{3' \rightarrow 1'} & t_{3' \rightarrow 2'} & \xi_{1,3'} & 0 & 0 & t_{1 \rightarrow 2} & 0 & 0 & t_{1 \rightarrow 3} \\ t_{2 \rightarrow 1} & 0 & 0 & \xi_{2,1'} & t_{1' \rightarrow 2'} & t_{1' \rightarrow 3'} & t_{2 \rightarrow 3} & 0 & 0 \\ 0 & t_{2 \rightarrow 1} & 0 & t_{2' \rightarrow 1'} & \xi_{2,2'} & t_{2' \rightarrow 3'} & 0 & t_{2 \rightarrow 3} & 0 \\ 0 & 0 & t_{2 \rightarrow 1} & t_{3' \rightarrow 1'} & t_{3' \rightarrow 2'} & \xi_{2,3'} & 0 & 0 & t_{2 \rightarrow 3} \\ t_{3 \rightarrow 1} & 0 & 0 & t_{3 \rightarrow 2} & 0 & 0 & \xi_{3,1'} & t_{1' \rightarrow 2'} & t_{1' \rightarrow 3'} \\ 0 & t_{3 \rightarrow 1} & 0 & 0 & t_{3 \rightarrow 2} & 0 & t_{2' \rightarrow 1'} & \xi_{3,2'} & t_{2' \rightarrow 3'} \\ 0 & 0 & t_{3 \rightarrow 1} & 0 & 0 & t_{3 \rightarrow 2} & t_{3' \rightarrow 1'} & t_{3' \rightarrow 2'} & \xi_{3,3'} \end{pmatrix} = \begin{pmatrix} H(1)_{1',3'} & H_{1,2} & H_{1,3} \\ H(1)_{2,1} & H(2)_{1',3'} & H_{2,3} \\ H_{3,1} & H_{3,2} & H(3)_{1,3'} \end{pmatrix} \quad (9)$$

with diagonal elements $[\xi_{1,1'}, \xi_{1,2'}, \xi_{1,3'}], [\xi_{2,1'}, \xi_{2,2'}, \xi_{2,3'}], [\xi_{3,1'}, \xi_{3,2'}, \xi_{3,3'}]$ set to $[(E_{p1} + E_{p1'} + E_c(1, 1')), (E_{p1} + E_{p2'} + E_c(1, 2')), (E_{p1} + E_{p3'} + E_c(1, 3'))], [(E_{p1} + E_{p1'} + E_c(1, 1')), (E_{p2} + E_{p2'} + E_c(2, 2')), (E_{p2} + E_{p3'} + E_c(2, 3'))], [(E_{p3} + E_{p1'} + E_c(3, 1')), (E_{p3} + E_{p2'} + E_c(3, 2')), (E_{p3} + E_{p3'} + E_c(3, 3'))]$. In the absence of magnetic field, we have $t_{k \rightarrow m} = t_{m \rightarrow k} = t_{k,l} = t_{m,k} \in \mathbf{R}$ and in the case of nonzero magnetic field $t_{k,m} = t_{m,k}^* \in \mathbf{C}$. It is straightforward to determine the matrix of two lines with N wells [=3 in this work] each following the mathematical structure of two interacting lines with three wells in each line. Matrices $H_{1,2}, H_{2,3}, H_{1,3}$ are diagonal of size $N \times N$ with all the same terms on the diagonal. At the same time, matrices $H(1)_{1',N'}, \dots, H(N)_{1',N'}$ have only different diagonal terms corresponding to $((\xi_{1,N'}, \dots, \xi_{1,N'}), \dots, ((\xi_{N,N'}, \dots, \xi_{N,N'}))$ elements. In simplified considerations we can set $t_{1 \rightarrow N} = t_{N \rightarrow 1}$ and $t_{1' \rightarrow N'} = t_{N' \rightarrow 1'}$ to zero since a probability for the wavefunction transfer from 1st to N -th lattice point is generally proportional to $\approx \exp(-sN)$, where s is some constant. It shall be underlined that in the most general case of two capacitively coupled symmetric SELs with three wells each (being parallel to each other), we have six (all different E_{pk} and $E_{pl'}$) plus 6 (all different $t_{k \rightarrow s}, t_{k' \rightarrow s'}$) plus three geometric parameters (d, a and b) as well as a dielectric constant hidden in the effective charge of interacting electrons q . Therefore, the model Hamiltonian has 13 real-valued parameters. They can be extracted from a particular transistor implementation of two SELs (Fig. 2C).

III. ANALYTICAL AND NUMERICAL MODELING OF CAPACITIVELY COUPLED SELS

A. Analytical Results

The greatest simplification of matrix 8 is when we set all $t_{k' \rightarrow m'} = t_{o \rightarrow m} = |t|$, and all $E_{pk} = E_{pm'} = E_p$ for $N=3$. Let us first consider the case of two insulating lines (all wells on each line are completely decoupled so there is no electron tunneling between the barriers and the barrier energies are high) where there are trapped electrons so $|t| = 0$ (electrons are confined in quantum wells and cannot move towards neighbouring wells). In such a case, we deal with

a diagonal matrix that has three different eigenvalues on its diagonal and has three different eigenenergy values

$$\begin{cases} E_1 = q_1 = E_p + \frac{e^2}{4\pi\epsilon\epsilon_0 d}, \\ E_2 = q_2 = E_p + \frac{e^2}{4\pi\epsilon\epsilon_0 \sqrt{|d|^2 + (a+b)^2}}, \\ E_3 = q_3 = E_p + \frac{e^2}{4\pi\epsilon\epsilon_0 \sqrt{|d|^2 + 4(a+b)^2}}, \end{cases}$$

so $E_3 < E_2 < E_1$. In the limit of infinite distance between SELs, we have nine degenerate eigenenergies. They are set to E_{pk} which corresponds to six decoupled quantum systems (the first electron is delocalized into three upper wells, while the second electron is delocalized into three lower wells).

Let us also consider the case of ideal metal where electrons are completely delocalized. In such a case, all $t_{k(k')} \gg E_{pl(s)}$ which brings Hamiltonian diagonal terms to be negligible in comparison with other terms. In such a case, we can set all diagonal terms to be zero which is an equivalent to the case of infinitely spaced SELs lines. It simply means that in the case of ideal metals, two lines are not 'seeing' each other.

Let us now turn to the case where processes associated with hopping between wells have similar values of energy to the energies denoted as $E_{pk(l')}$. In such a case, the Hamiltonian matrix can be parametrized only by three real value numbers due to symmetries depicted in Fig. 2B (we divide the matrix by a constant number $|t|$) so

$$\begin{cases} q_{11} = \frac{2E_p + \frac{e^2}{d}}{|t|}, \\ q_{12} = \frac{2E_p + \frac{e^2}{\sqrt{d^2 + (a+b)^2}}}{|t|}, \\ q_{13} = \frac{2E_p + \frac{e^2}{\sqrt{d^2 + 4(a+b)^2}}}{|t|}. \end{cases}$$

For a fixed $|t|$, we change the distance d and observe that q_{11} can be arbitrary large, while q_{12} and q_{13} have finite values for $d=0$. Going into the limit of infinite distance d , we observe that all q_{11}, q_{12} and q_{13} approach a finite value $\frac{2E_p}{|t|}$. We obtain the

simplified Hamiltonian matrix that is a Hermitian conjugate and has a property $H_{k,k} = H_{N-k+1,N-k+1}$. It is in the form

$$\hat{H} = \begin{pmatrix} q_{11} & 1 & 0 & 1 & 0 & 0 & 0 & 0 & 0 \\ 1 & q_{12} & 1 & 0 & 1 & 0 & 0 & 0 & 0 \\ 0 & 1 & q_{13} & 0 & 0 & 1 & 0 & 0 & 0 \\ 1 & 0 & 0 & q_{12} & 1 & 0 & 1 & 0 & 0 \\ 0 & 1 & 0 & 1 & q_{11} & 1 & 0 & 1 & 0 \\ 0 & 0 & 1 & 0 & 1 & q_{12} & 0 & 0 & 1 \\ 0 & 0 & 0 & 1 & 0 & 0 & q_{13} & 1 & 0 \\ 0 & 0 & 0 & 0 & 1 & 0 & 1 & q_{12} & 1 \\ 0 & 0 & 0 & 0 & 0 & 1 & 0 & 1 & q_{11} \end{pmatrix} \quad (10)$$

We can analytically find nine energy eigenvalues and they correspond to the entangled states. We have

$$\begin{cases} E_1 = q_{11}, \\ E_2 = q_{12}, \\ E_3 = \frac{1}{2}(q_{11} + q_{12} - \sqrt{8 + (q_{11} - q_{12})^2}), \\ E_4 = \frac{1}{2}(q_{11} + q_{12} + \sqrt{8 + (q_{11} - q_{12})^2}), \\ E_5 = \frac{1}{2}(q_{12} - q_{13} - \sqrt{8 + (q_{12} - q_{13})^2}), \\ E_6 = \frac{1}{2}(q_{12} - q_{13} + \sqrt{8 + (q_{12} - q_{13})^2}). \end{cases} \quad (11)$$

The last 3 energy eigenvalues are the most involving analytically and are the roots of a 3rd order polynomial

$$2q_{11} + 6q_{13} - q_{11}q_{12}q_{13} + (-8 + q_{11}q_{12} + q_{11}q_{13} + q_{12}q_{13})E_k - (q_{11} + q_{12} + q_{13})E_k^2 + E_k^3 = 0 \quad (12)$$

We omit writing direct and very lengthy formulas since the solutions of a 3rd-order polynomial are commonly known. The eigenvectors have the structure given in Appendix.

We can readily recognize that all nine energy eigenvectors are entangled. In particular, $|E_1\rangle = |1, 0, 0\rangle_u |1, 0, 0\rangle_l - |0, 1, 0\rangle_u |0, 1, 0\rangle_l + |0, 0, 1\rangle_u |0, 0, 1\rangle_l$ or $|E_2\rangle = |1, 0, 0\rangle_u |0, 1, 0\rangle_l - |0, 1, 0\rangle_u |1, 0, 0\rangle_l - |0, 1, 0\rangle_u |0, 0, 1\rangle_l + |0, 0, 1\rangle_u |0, 1, 0\rangle_l$, so they have no equivalence in the classical picture of two charged balls in channels that are repelling each other.

B. Numerical Results for Case of Capacitively Coupled SETs

At first we are analyzing available spectrum of eigenenergies as in the case of insulator-to-metal phase transition, which can be implemented in a tight-binding model by a systematic increase of the hopping term from small to large values, while at the same time keeping all other parameters constant, as depicted in Fig.2.

The numerical modeling of electron transport across coupled SELs is about solving a set of nine coupled recurrent equations of motion. We can recognize that probability of occupancy of $(1,1')$ given by $|\gamma_1(t)|^2$ (two electrons as SELs inputs) can be compared with occupancy of $(3,3')$ by $p_9 = |\gamma_9(t)|^2$ (2 electrons at SELs outputs) as depicted in Fig.3. We can also compare the situation of measurement of only one electron at the output of each line that is given by the output of first upper SEL that is correlated

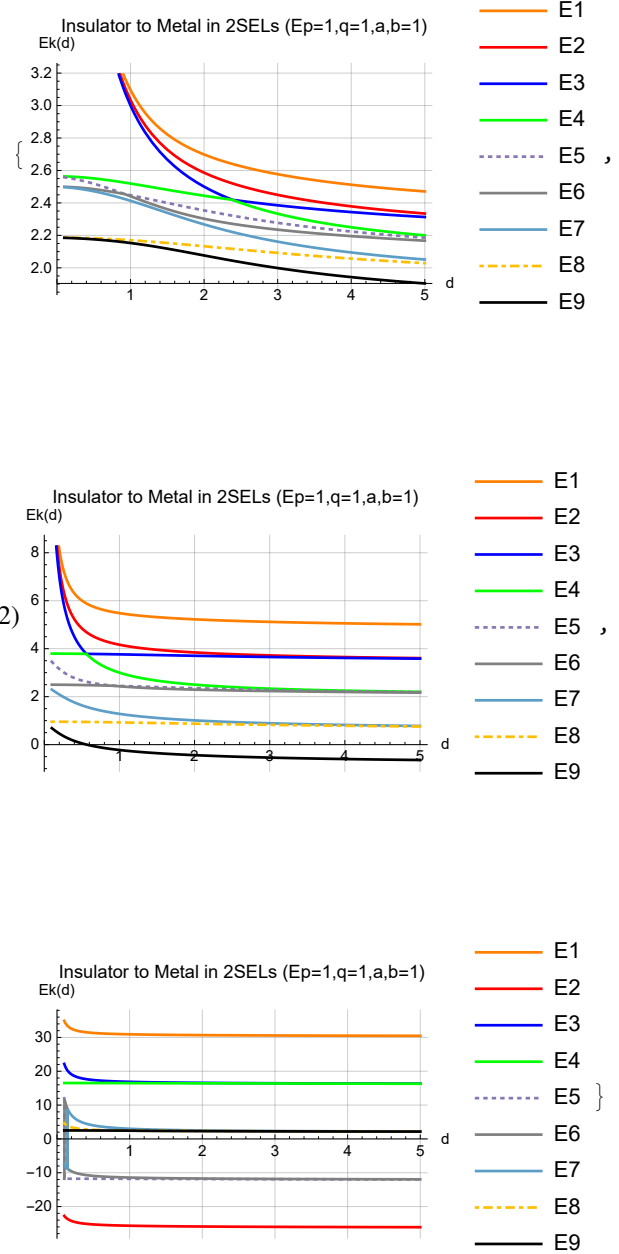


Fig. 2. Transition from insulator (upper) to metallic state (bottom) given by eigenenergy spectra as function of distance between two single electron lines. Different hopping terms were used $t = (0.01, 0.1, 1)$ [from top to bottom plots] and $e=1$.

with $p_7 = |\gamma_7(t)|^2$ (that spans the state $|0, 0, 1\rangle_u |1, 0, 0\rangle_l$) or to $p_8 = |\gamma_8(t)|^2$ (that spans the state $|0, 0, 1\rangle_u |0, 1, 0\rangle_l$). Alternatively, we can consider the one electron output of the second line while there is no electron at the output of the first line, which corresponds to $\gamma_3(t)$ spanning the state $|1, 0, 0\rangle_u |0, 0, 1\rangle_l$ or to the coefficient $\gamma_6(t)$ spanning the state $|0, 1, 0\rangle_u |0, 0, 1\rangle_l$.

C. Act of Measurement and Dynamics of Quantum State over Time

The quantum system dynamics over time is expressed by the equation of motion $\hat{H}(t') |\psi(t')\rangle = i\hbar \frac{d}{dt'} |\psi(t')\rangle$ that can be represented in discrete time step by relation

$$\frac{dt'}{i\hbar} \hat{H}(t') |\psi(t')\rangle + |\psi(t')\rangle = |\psi(t' + dt')\rangle. \quad (13)$$

It leads to the following equations of motion for quantum state expressed by equation (8) as follows

$$\vec{\gamma}(t' + dt) = \begin{cases} \gamma_1(t' + dt) = \gamma_1(t') + dt' \sum_{k=1}^9 \hat{H}_{1,k}(t') \gamma_k(t') = f_1(\vec{\gamma}(t'), dt') [\hat{H}(t')], \\ \dots \\ \gamma_9(t' + dt) = \gamma_9(t') + dt' \sum_{k=1}^9 \hat{H}_{9,k}(t') \gamma_k(t') = f_9(\vec{\gamma}(t'), dt') [\hat{H}(t')] \end{cases} = \vec{f}(\vec{\gamma}(t'), dt') [\hat{H}(t')]. \quad (14)$$

The measurement can be represented by projection operators $\hat{\Pi}(t')$ equivalent to the matrix that acts on the quantum state over time. The lack of measurement can simply mean that the state projects on itself so the projection is the identity operation ($\hat{\Pi}(t') = \hat{I}_{9 \times 9}$). Otherwise, the quantum state is projected on its subset and hence the projection operator can change in a non-continuous way over time. We can formally write the quantum state dynamics with respect to time during the occurrence of measurement process (interaction of external physical system with the considered quantum system) as

$$\vec{\gamma}(t' + dt') = \frac{\hat{\Pi}(t' + dt') (\vec{f}(\vec{\gamma}(t'), dt') [\hat{H}(t')])}{(\hat{\Pi}(t' + dt') \vec{f}(\vec{\gamma}(t'), dt') [\hat{H}(t')])^\dagger (\hat{\Pi}(t' + dt') \vec{f}(\vec{\gamma}(t'), dt') [\hat{H}(t')])}. \quad (15)$$

Let us refer to some example by assuming that a particle in the upper SELs was detected by the upper output detector (Fig. 1b). In such a case, the following projector $\hat{\Pi}(t, t + \Delta t)$ is different from the identity in time interval $(t, t + \Delta t)$ with $1_{1,t,t+\Delta t} = 1$ set to 1 in this time interval and 0 otherwise. The projector acts on the quantum state (diagonal matrix is given by diag symbol). It is given as

$$\begin{aligned} \hat{\Pi}(t, t + \Delta t) &= (1 - 1_{t,t+\Delta t})(\hat{I}_U \times \hat{I}_L) + 1_{t,t+\Delta t}(|0, 0, 1\rangle_U \langle 0, 0, 1|_U \times \hat{I}_L) = \\ &= (1 - 1_{t,t+\Delta t})(\hat{I}_U \times \hat{I}_L) + 1_{t,t+\Delta t}(|0, 0, 1\rangle_U \langle 0, 0, 1|_U \times (|1, 0, 0\rangle_L \langle 1, 0, 0|_L + |0, 1, 0\rangle_L \langle 0, 1, 0|_L + |0, 0, 1\rangle_L \langle 0, 0, 1|_L)) = \\ &= (1 - 1_{t,t+\Delta t})\hat{I}_{9 \times 9} + 1_{t,t+\Delta t} \text{diag}(0, 0, 1) \times \hat{I}_{3 \times 3} = \\ &= \text{diag}((1 - 1_{t,t+\Delta t}), (1 - 1_{t,t+\Delta t}), (1 - 1_{t,t+\Delta t}), (1 - 1_{t,t+\Delta t}), (1 - 1_{t,t+\Delta t}), (1 - 1_{t,t+\Delta t}), (1 - 1_{t,t+\Delta t}), 1, 1, 1) \end{aligned} \quad (16)$$

So far, the conducted analysis is based on a tight-binding approximation expressed by formula (8). It uses only one lattice point for the description of particle presence in the quantum well that is a continuous object and consists of an infinite number of points as given by the Schrödinger equations of motion. We can move from discrete mathematics into continuous analysis by using a Wannier function representation of equation (8). We have to transfer from term $|1, 0, 0\rangle_U |1, 0, 0\rangle_U$ (or $|r\rangle_U |s\rangle_U$) into $w_1(x_U)w_1(x_L)$ (or $w_r(x_U)w_s(x_L)$), so we can obtain a quantum state in the form of a two-particle wavefunction

$$\begin{aligned} |\psi(x_U, x_L, t)\rangle &= \gamma_1(t)w_1(x_U)w_1(x_L) + \gamma_2(t)w_1(x_U)w_2(x_L) + \gamma_3(t)w_1(x_U)w_3(x_L) + \gamma_4(t)w_2(x_U)w_1(x_L) \\ &+ \gamma_5(t)w_2(x_U)w_2(x_L) + \gamma_6(t)w_2(x_U)w_3(x_L) + \gamma_7(t)w_3(x_U)w_1(x_L) + \gamma_8(t)w_3(x_U)w_2(x_L) + \gamma_9(t)w_3(x_U)w_3(x_L), \end{aligned} \quad (17)$$

where $w_k(x_{U(L)})$ are maximum-localized quantum states given in the form of Wannier functions [6] (that are linear combinations of Hamiltonian energy eigefunctions) at subsequent Up (U)/Lower (L) quantum wells depicted in Fig. 1. It is important to underline that the tight-binding model allows for a quick detection of entangled states and for a transfer of this information into Schrödinger formalism, which has its importance in the design of quantum computer consisting of many coupled entangled qubits (fundamental modelling due to the large Hilbert space is limited to 10 qubits). Quite obviously, the Schrödinger equation gives detailed space resolution of quantum mechanical phenomena taking place in 2 or N electrostatically coupled SELs that might contain an arbitrary number of quantum wells. Incorporation of spin effects is also possible in the given framework, but is beyond the scope of this work.

IV. CONCLUSION

The tight-binding model can be derived from the Schrödinger formalism (and vice versa) and is the simplistic version of the Hubbard model that is a very universal model capable of describing various collective phenomena in condensed matter physics. Therefore, it is expected that the tight-binding model can be also effective in describing physical effects in various CMOS nanostructures. In the presented work, new qualitative features of two capacitively coupled single-electron lines were described as occupancy oscillations at SELs nodes given by Fig. 3. Obtained occupancy oscillations do not occur in the classically coupled electrical lines and thus are the feature of quantumness of the studied structure. From obtained solutions we can spot the possible transitions between energy levels when the system is subjected to the external microwave field as coming from RF sources

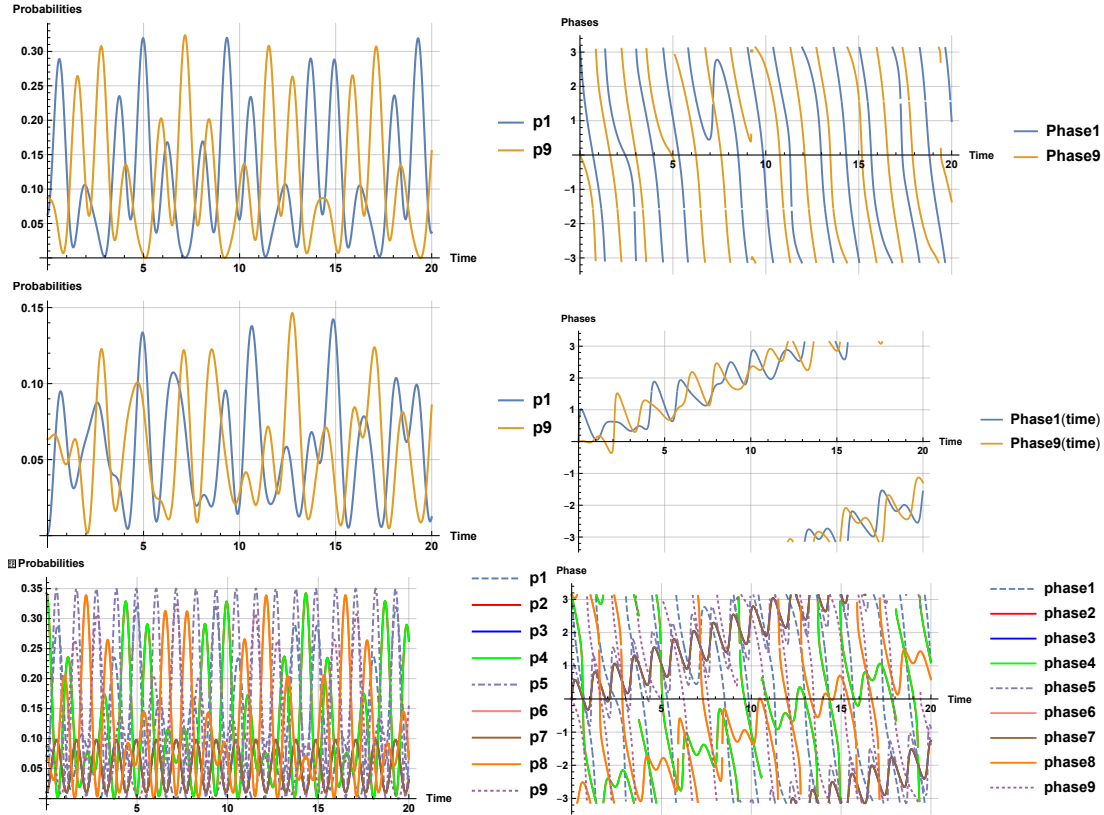


Fig. 3. Two SELs over time: Upper plots populate 3 energy levels, while other plots correspond to occupancy of 9 energy levels. Left plots describe the correlations between probabilities of finding both electrons simultaneously at the input and output. Evolution of two two-body quantum-state phases (from $\gamma_1(t)$ and $\gamma_9(t)$) is given in equation (8). Right plots point out probabilities of finding electrons in all 9 possible configurations in 2SELs (Fig. 1) with time and phases of $(\gamma_1(t), \dots, \gamma_9(t))$.

placed in the proximity of SELs. The conducted study has its relevance in single-electron transistor structures as deriving from nanoscale CMOS. Such systems are expected to mimic various types of programmable quantum matter that can simulate many types of physical phenomena. One of the interesting case is the imitation of metal-insulator phase transition in coupled nanowires as given in Fig. 2 that can be obtained with electrical tuning of 2-SELs system. It shall be also underlined that the described position-dependent qubits are analogical to superconducting Cooper pair boxes where quantum phase transitions have been observed [3], [7]. The hopping term in the tight-binding model of semiconductor position-dependent qubits is analogical to energy of Josephson coupling in superconducting Cooper pair box (or in other types of superconducting qubits). Therefore, the existence of quantum phase transitions [9] is expected to occur in the studied SELs system as quantum phase transitions occurs in arrays of electrostatically coupled Josephson junctions.

In a future work using the tight-binding model, one is expected to observe the classical properties of capacitively coupled lines when one moves from quantum situation of very few electric charges into the case of long lines with N wells, where there are m electrons at each line and when the number of electrons goes into infinity (i.e. transition from the quantum to classical picture). Another example is the repulsion (anticorrelation in position) of two electrons at two parallel SELs that can be used in the construction of quantum SWAP gate. Therefore, the results obtained analytically and numerically on the two interacting SELs has its meaning in the development of quantum technologies [5] and also point to the interlink between the fundamental and applied science.

We would like to thank to Adam Bednorz from University of Warsaw for fruitful discussions and remarks. This work was supported by Science Foundation Ireland under Grant 14/RP/I2921.

V. APPENDIX

The simplified Hamiltonian (also given by equation 10) for 2 electrostatically interacting Single Electron Lines (Fig.1.) has eigenvalues pointed by formulas (10)-(12) and has following matrix and its eigenvectors

$$\hat{H} = \begin{pmatrix} q_{11} & 1 & 0 & 1 & 0 & 0 & 0 & 0 & 0 \\ 1 & q_{12} & 1 & 0 & 1 & 0 & 0 & 0 & 0 \\ 0 & 1 & q_{13} & 0 & 0 & 1 & 0 & 0 & 0 \\ 1 & 0 & 0 & q_{12} & 1 & 0 & 1 & 0 & 0 \\ 0 & 1 & 0 & 1 & q_{11} & 1 & 0 & 1 & 0 \\ 0 & 0 & 1 & 0 & 1 & q_{12} & 0 & 0 & 1 \\ 0 & 0 & 0 & 1 & 0 & 0 & q_{13} & 1 & 0 \\ 0 & 0 & 0 & 0 & 1 & 0 & 1 & q_{12} & 1 \\ 0 & 0 & 0 & 0 & 0 & 1 & 0 & 1 & q_{11} \end{pmatrix}, |E_1\rangle = \begin{pmatrix} 1, \\ 0, \\ 0, \\ 0, \\ -1, \\ 0, \\ 0, \\ 0, \\ 1 \end{pmatrix}, |E_2\rangle = \begin{pmatrix} 0, \\ 1, \\ 0, \\ -1, \\ 0, \\ -1, \\ 0, \\ 1, \\ 0 \end{pmatrix}, \quad (18)$$

$$|E_3\rangle = \begin{pmatrix} -1, \\ \frac{1}{4}(q_{11} - q_{12} + \sqrt{8 + (q_{11} - q_{12})^2}), \\ 0, \\ \frac{1}{4}(q_{11} - q_{12} + \sqrt{8 + (q_{11} - q_{12})^2}), \\ 0, \\ -\frac{1}{4}(q_{11} - q_{12} + \sqrt{8 + (q_{11} - q_{12})^2}), \\ 0, \\ -\frac{1}{4}(q_{11} - q_{12} + \sqrt{8 + (q_{11} - q_{12})^2}), \\ 1 \end{pmatrix}, |E_4\rangle = \begin{pmatrix} -1, \\ \frac{1}{4}(q_{11} - q_{12} - \sqrt{8 + (q_{11} - q_{12})^2}), \\ 0, \\ \frac{1}{4}(q_{11} - q_{12} - \sqrt{8 + (q_{11} - q_{12})^2}), \\ 0, \\ -\frac{1}{4}(q_{11} - q_{12} - \sqrt{8 + (q_{11} - q_{12})^2}), \\ 0, \\ -\frac{1}{4}(q_{11} - q_{12} - \sqrt{8 + (q_{11} - q_{12})^2}), \\ 1 \end{pmatrix}, \quad (19)$$

$$|E_5\rangle = \begin{pmatrix} -1, \\ \frac{1}{4}(q_{12} - q_{13} + \sqrt{8 + (q_{12} - q_{13})^2}), \\ 0, \\ \frac{1}{4}(q_{12} - q_{13} + \sqrt{8 + (q_{12} - q_{13})^2}), \\ 0, \\ -\frac{1}{4}(q_{12} - q_{13} + \sqrt{8 + (q_{12} - q_{13})^2}), \\ 0, \\ -\frac{1}{4}(q_{12} - q_{13} + \sqrt{8 + (q_{12} - q_{13})^2}), \\ 1 \end{pmatrix}, |E_6\rangle = \begin{pmatrix} -1, \\ \frac{1}{4}(q_{12} - q_{13} - \sqrt{8 + (q_{12} - q_{13})^2}), \\ 0, \\ \frac{1}{4}(q_{12} - q_{13} - \sqrt{8 + (q_{12} - q_{13})^2}), \\ 0, \\ -\frac{1}{4}(q_{12} - q_{13} - \sqrt{8 + (q_{12} - q_{13})^2}), \\ 0, \\ -\frac{1}{4}(q_{12} - q_{13} - \sqrt{8 + (q_{12} - q_{13})^2}), \\ 1 \end{pmatrix}, \quad (20)$$

$$|E_{k=(7..9)}\rangle = \begin{pmatrix} 1, \\ (E_{k=(7..9)} - q_{11})/2, \\ \frac{(-E_{k=(7..9)} + q_{11})(-2 + E_{k=(7..9)}^2 + q_{11}q_{12} - E_{k=(7..9)}(q_{11} + q_{12}))}{2(-3E_{k=(7..9)} + q_{11} + 2q_{13})}, \\ (E_{k=(7..9)} - q_{11})/2, \\ 2, \\ (E_{k=(7..9)} - q_{11})/2, \\ 2, \\ \frac{(-E_{k=(7..9)} + q_{11})(-2 + E_{k=(7..9)}^2 + q_{11}q_{12} - E_{k=(7..9)}(q_{11} + q_{12}))}{2(-3E_{k=(7..9)} + q_{11} + 2q_{13})} \end{pmatrix}. \quad (21)$$

REFERENCES

- [1] K.Pomorski, H.Akaike, A.Fujimaki, and K.Rusek. Relaxation method in description of ram memory cell in rsfq computer. COMPEL, 38(1):395414, 2019
- [2] B.Patra, R.Incandela, J.Van Dijk, H.Homulle, L.Song, M.Shahmohammadi, R.B.Staszewski, and et al. Cryo-emos circuits and systems for quantum computing applications. IEEE Journal of Solid-State Circuits, 53(1):309321, 2018.
- [3] M.-S. Choi, J. Yi, M. Y. Choi, J. Choi, and S.-I. Lee. Quantum phase transitions in josephson-junction chains. Phys. Rev. B, 57:R716R719, 1998.
- [4] T. Fujisawa, T. Hayashi, HD Cheong, YH Jeong, and Y. Hirayama. Rotation and phase-shift operations for a charge qubit in a double quantum dot. Physica E: Low-dimensional Systems and Nanostructures, 21(2-4):10461052, 2004.
- [5] P. Giouanlis, E. Blokhina, D. Leipold, and R. B. Staszewski. Occupancy oscillations and electron transfer in multiplequantumdot qubits and their circuit representation. In Proceedings of ICECS, pages 14. IEEE, 2018.
- [6] P. Giouanlis, E. Blokhina, K. Pomorski, D. R. Leipold, and R. B. Staszewski. Modeling of semiconductor electrostatic qubits realized through coupled quantum dots. IEEE Access, pages 116, 2019.
- [7] D. Maile, S. Andergassen, and W. Belzig. Quantum phase transition with dissipative frustration. Phys. Rev. B, 97, 2018.
- [8] K. D. Petersson, J. R. Petta, H. Lu, and A. C. Gossard. Quantum coherence in a one-electron semiconductor charge qubit. Phys. Rev. Lett., 105:246804, 2010.
- [9] S.Sachdev. Quantum phase transitions. Cambridge Univ. Press, 2011.
- [10] H. Q. Xu. Method of calculations for electron transport in multiterminal quantum systems based on real-space lattice models. Phys. Rev. B, 66:165305, 2002.